EGYPTIAN PHARMACEUTICAL JOURNAL EPJ Original Article 21

# Silver and titanium dioxide nanoparticles bullets against multi-drug-resistant gram-negative urine-bacteria beside their antineoplastic activity to HepG2 cell line

Ahmed Abdallah[1], Ahmed N. Emam[2,3], Eslam S. Abdelmouty[1], Emad A. Ewais[1], Mohamed Khedr[1 *]

[1]Botany and Microbiology Department, Faculty of Science, Al-Azhar University, Nasr City, Cairo, 11884, Egypt
[2]Refractories, Ceramics and Building Materials Department, Advanced Materials Technology & Mineral Resources Research Institute, National Research Centre (NRC), El Bohouth St., Dokki, 12622 Cairo, Egypt.
[3]Nanomedicine & Tissue Engineering Research Lab, Medical Research Centre of Excellence, National Research Centre, El Bohouth St., Dokki, 12622 Cairo, Egypt
[*]Corresponding author: Dr. Mohamed Khedr, PhD, Botany and Microbiology Department, Faculty of Science, Al-Azhar University, Nasr City, Cairo, 11884, Egypt
ORCID ID: 0000-0001-6118-8607
E-mail mohamedkhedr.221@Azhar.edu.eg

**Received:** 10 December 2024
**Revised:** 2 January 2025
**Accepted:** 6 January 2025
**Published:** 23 April 2025

**Egyptian Pharmaceutical Journal** 2025, 24: 21-32

**Background**
Multidrug-resistant (MDR) bacteria are a fundamental risk and cause of fatal chronic infections. Objectives: Evaluate Silver and Titanium NPs antibacterial activity in addition to their anticancer potential against HepG2 cell line.
**Materials and methods**
The nanoparticles were characterized after their synthesis by investigating their optical, morphological structure, and colloidal properties using UV-Vis absorption spectral analysis, transmission electron microscopy (TEM), X-ray diffraction analysis (XRD), and dynamic light scattering (DLS) techniques**.**
**Results**
The present study characterized twenty-two isolated bacterial species as MDR strains based on their resistance to antibiotic examinations. It tested the antibacterial activity of silver (AgNPs) and titanium dioxide ($TiO_2$NPs) nanoparticles against urinary tract bacterial strains. The average particle size of AgNPs and $TiO_2$NPs was 30±5, and 20±5 nm with cubic and anatase crystal structures, respectively. AgNPs showed a minimal inhibition concentration (MIC) within the range of 4 to 8 µg/mL, which is lower than $TiO_2$NPs ranging from 500 to 1000 µg/mL. Also, AgNPs are the most effective antimicrobials, with inhibition zones between 31 and 33 mm wide and cover ten different types of Klebsiella pneumonia. On the other hand, $TiO_2$NPs showed remarkable antibacterial efficacy against MDR isolates with inhibition zones of about 31–33 mm. The most extensive MDR bacterial strains were *Klebsiella pneumonia*A031 [OP811040] and *Klebsiella pneumonia*A065 [OP811041]. $TiO_2$NPs had less toxicity on the same types of HepG-2 cells, than Ag NPs as toxicity appeared at a concentration higher than 125 µg/ml; it was 3.2% at 250 µg/ml, then 28.2% at 500 µg/ml, and finally 90.2% at 1000 µg/ml.
**Conclusion**
our results investigate promising antibacterial and anticancer activity of two prepared Ag and $TiO_2$NPs particularly against *Klebsiella pneumonia* and HepG2 cell line.

**Keywords:** Silver Nanoparticles, Titanium Nanoparticles, multi-drug resistance bacterial isolates, urinary tract infection, HepG2 cell line
Egypt Pharmaceut J. 24:21–32

1687-4315

## Introduction

One of the most significant public health concerns of our day, in the opinion of many, is multidrug-resistant (MDR) bacteria. The Infectious Diseases Society of America (IDSA) has declared that "one of the most serious threats to human wellness worldwide" is antimicrobial resistance [1]. The emergence of MDR microbes poses a significant threat for several reasons. To begin with, MDR bacterial infections are generally worse than infections from more susceptible organisms [2, 3]. As a result, increasing rates of antibiotic resistance influence many sides of contemporary medicine and jeopardize the efficacy of many medical breakthroughs, such as surgery, organ transplantation, and cancer treatment. Second, these infections come with hefty added expenses. Third, there is a strong correlation between the use of antibiotics with a wide spectrum for both empirical and final treatment, as well as the presence of some MDR bacteria [4]. The increased prevalence of MDR bacteria due to improper use creates a vicious cycle. Urinary tract infections (UTIs) rank several common infectious disorders. They are also the

second most common reason doctors prescribe antibiotics in many hospitals, with respiratory infections coming in first. *E. coli*, the most frequently mentioned etiology, accounts for 90% of urinary tract infections with normal anatomy and unblocked urinary tracts [5]. UTIs are rare in men under 50 but common in those over 50. When administered correctly, antibiotics easily treat urinary tract infections [6]. All urinary tract infections (UTIs) are typically complicated because they have spread to the upper urinary tract. As a result, we can better manage male UTIs using culture and analysis of antibiotic susceptibility patterns, which aid in modifying treatment plans [7, 8]. In this case, we used empirical antibiotics such as levofloxacin, ciprofloxacin, Fosfomycin, or nitrofurantoin to treat urinary tract infections. But because MDR pathogens keep coming out, we now treat patients with lactams, fluoroquinolones, trimethoprim-sulfamethoxazole, amoxicillin-clavulanic acid, or a third-generation cephalosporin until we get a culture that is sensitive [9, 10]. However, these bacteria could form biofilms, leading to difficult-to-treat infections, extended hospital stays, and expensive medical bills [11].

As a result, the continued emergence of antibiotic-resistant bacteria and their propensity to form biofilms pose challenges to infection therapy. Consequently, developing novel, effective therapy options to prevent and treat UTIs successfully is a scientific challenge. For example, metallic and metal oxide nanoparticles can stop biofilm formation, break down multidrug resistance, and direct drugs to where they need to work while preventing healthy cells from going through cytotoxic processes. The antimicrobial properties of metals, metal oxide, and surface-tailored nanocarriers have enabled these advancements in treating UTIs [12].

Nanoparticle fabrication and attachment to antimicrobials can produce long-lasting, cost-effective, and synergistic antibacterial effects [13, 14]. Metals, like silver nanoparticles (AgNPs), and metal-based oxides, like zinc oxide (ZnONPs) and Titanium dioxide ($TiO_2$NPs), are the most widely used antimicrobial nanoparticles (NPs) for urinary tract infections [12, 15-20]. There are several photo-thermolysis processes that all metallic and metal-based oxide nanoparticles use to hurt pathogenic bacteria. These include making reactive oxygen species (ROS) and killing pathogen cells. This can lead to the disruption of regular enzymatic activity, DNA synthesis, and the integrity of cell walls and components [21, 22]. Silver (Ag1+) ions could cling to the cell wall and cytoplasmic membrane. Adherent ions could increase the membrane's cytoplasmic permeability and disturb the stability of the bacterial sheath [23, 24]. When free Ag1+ enters cells, it inhibits respiratory enzymes and produces reactive oxygen species while blocking the synthesis of adenosine triphosphate [23]. In microorganisms, ROS are the leading cause of cell membrane rupture and DNA modification [24]. Furthermore, nanoparticles have the potential to dephosphorylate tyrosine residues on protein substrates, and the process of protein substrate phosphorylation affects bacterial signal transduction. These are two more potential roles for AgNPs in bacterial signaling. Interference with signal transduction can halt cell division and apoptosis [25]. However, $TiO_2$NPs are highly sought after for antimicrobial uses because they have special qualities such as the ability to clean themselves, being safe, and having photocatalytic activity that kills bacteria [26, 27]. High oxidative potential (ROS) commonly links $TiO_2$NPs to their antimicrobial properties. When O2 is present, band-gap irradiation photo-increases charge, which makes ROS and stops the formation of lipid peroxidation or O-singlets. By changing several crucial structures (such as the cell wall, membrane, DNA, etc.) and metabolic pathways, such a free radical set of redox events can result in cell death [28].

In this study, we aim to combine, describe, and compare how well AgNPs and $TiO_2$NPs kill bacteria and MDR *Klebsiella pneumonia* strains from urology patients at Mansura University Hospital. We also want to see how well synthesized NPs kill cancer cells from the hepatocarcinoma cell line. This multifaceted approach will let us not only test how well silver nanoparticles (AgNPs) and titanium dioxide nanoparticles ($TiO_2$NPs) kill microbes but also investigate their potential as therapeutic agents to fight both cancer cell growth and bacterial resistance. By conducting comprehensive assays, we hope to elucidate the underlying mechanisms of action and pave the way for novel treatment strategies.

## Materials and methods

### Materials

Tetra-isopropyl ortho-titanate (TIOT, $Ti[OCH(CH_3)_2]_4$, 99.5%) is purchased from Sigma-Aldrich, Germany. Silver nitrate ($AgNO_3$) was purchased from Techno Pharm-Chem 99%. Sodium borohydride ($NaBH_4$, 85%,iis fromWinLab Ltd). Polyvinylpyrrolidone ($C6H_9NO$)n, PVP 40K, Alpha Chemika 99%). Isopropanol $(CH_3)_2CHOH$, EL-Gohoria Chemicals).Mueller-Hinton Agar (Oxoid Limited).

**Fabrication of silver (AgNPs) and titanium dioxide ($TiO_2$NPs) nanoparticles**

***Fabrication of silver nanoparticles (AgNPs)***

Spherical silver nanoparticles have been prepared using the chemical reduction method, with minor modifications to the procedure previously described by Ali et al. [16]. Specifically, a 100-mL aqueous solution having 0.047 M $AgNO_3$ into a 200-mL reaction vessel, vigorously stirring it in an ice bath under dark conditions. Next, we vigorously stirred the $AgNO_3$ solution to incorporate polyvinylpyrrolidone (PVP 40K). The molar ratio between $AgNO_3$ and PVP-40K was around 235.45. After 15 minutes, the reaction vessel received a dropwise addition of an ice-cooled 10 mM NaBH4 aqueous solution. The reaction underwent a color change from being colorless to a yellowish-brown hue because of the production of spherical AgNPs. The resulting colloidal suspension agitated for 1 h and then allowed it to mature for 24 h before using it.

**Preparation of titanium dioxide ($TiO_2$NPs) nanoparticles**

$TiO_2$NPs were synthesized using the sol-gel technique with minor adjustments, as mentioned elsewhere [29, 30]. In Typical synthesis, 10 mL of TIOT was submerged in 90 mL of 1-propanol at room temperature while being stirred vigorously. Next, using strong magnetic agitation, 10 ml of deionized water was gradually added to obtain pure Ti (OH)2. The resulting colloidal suspensions were stirred at room temperature for 4 h using a magnetic stirrer. When pure $Ti(OH)_2$ was utilized, white gels were produced. The yield gels were then dehydrated in a high-temperature oven set at 100°C for a duration of 12 h to remove the water. Ultimately, the powders were introduced into a muffle furnace and subjected to annealing for a duration of 4 h at a temperature of 500 °C, resulting in the creation of pure $TiO_2$NPs.

**Characterization**

The photophysical parameters, specifically UV-Vis absorption, were analyzed using a TG80 (PG instruments) double-beam UV-Vis spectrophotometer. The absorption spectra were recorded in the wavelength range of 250 to 900 nm. The structure of the silver nanoparticles was examined using high-resolution transmission electron microscopy (HR-TEM) JEM 2100 LB6, operating at a voltage of 160 kV. The crystallographic structure of the silver and titanium dioxide nanoparticles was analyzed using the Bruker D8 Discover, scanning from 35 to 90° with a step size of 0.01°. In addition, the colloidal properties, including the distribution of particle sizes and the zeta potential, were assessed using dynamic light scattering (DLS) using a Malvern Zeta sizer Nano-ZS (Malvern Instruments Ltd., Worcestershire, UK).

**Minimum inhibitory concentration test for silver and Titanium Nanoparticles**

The minimum inhibitory concentration (MIC) is defined as the drug's minimal concentration that will inhibit growth as measured by observed turbidity in the test tube [15]. The agar-well diffusion method found the smallest amount of AgNPs and $TiO_2$NPs that would stop the reaction from happening. A solution is composed of microbially mediated nanoparticles suspended in one milliliter of sterilized DDH2O and subjected to serial dilution from AgNPs and $TiO_2$NPs with concentrations ranging from 500 g/mL to 50 g/mL. Before the experiment, 20 mL of pre-solidified medium were used to prepare each Muller-Hinton agar plate, which was then allowed to cool at room temperature. The means of the sterilized swap was used to streak the five chosen MDR bacterial isolates (Abs = 0.5 at 600 nm) obtained from Urine samples onto the agar plates. A maximum of four wells per plate were made using sterilized plastic tip heads, and 50 µL of the nanoparticle-containing solution was added to each well independently. Following a 24-hour incubation period at 37°C for the cultures, the inhibition zone that formed around the wells was measured in millimeters to assess the antimicrobial activity of the nanoparticles [31, 32].

**Anticancer activity of AgNPs and $TiO_2$NPs against Hepatocarcinoma**

The American type culture collection (ATCC HB-8065) measured the anticancer activity of AgNPs and $TiO_2$NPs on the human tumor cell line (HepG2) using MTT (3,4,5-dimethylthiazol-2-yl)-2-5-diphenyl tetrazolium bromide. The mitochondrial dehydrogenase reduces MTT, forming a purple formazan compound [33]. The hepatocellular carcinoma line of cells (HepG2) was incubated at 37 °C in a 96-well plate for 24 h before the treatments. After incubation, the cell lines were subjected to different concentrations of AgNPs and $TiO_2$NPs (31.25, 62.5, 125, 250, 500, and 1000 µg/mL). Following the treatment, we carefully removed the content by aspiration, then added 100 mL of 0.5 mg mL-1 MTT in cell culture medium to each well and incubated for 2 hours. To dissolve the formed crystals of formazan, 100 mL of 10% (sodium dodecyl sulfate) SDS was applied. The amount of formazan was measured with a microplate reader at 560 nm [34].

**Statistical analysis**

The Xlstate 2020 program was used in all the previous studies that employed ANOVA and standard deviation, according to Mostafaei (2014) [33]. Therefore, these methods were used to analyze the data. [35].

## Results and Discussion

### Fabrications and characterizations of silver and titanium dioxide nanoparticles

In this study, $NaBH_4$, a reducing agent, chemically reduces silver salts (Ag+NO3-) to create spherical-shaped AgNPs. The steric effect of PVP's long polyvinyl chain stops aggregation and extra grain growth when it is used as a capping agent [16, 36, 37]. The synthesis of silver nanospheres produced a brownish-yellow colored solution. The adsorption of borohydride (BH4-) is critical in stabilizing the growth of AgNPs because it provides a charge to the particle surface [16, 36].

Figure 1 displays the optical characteristics of the spherical AgNPs in their original state. It reveals a single, narrow surface plasmon band (SPR) with a wavelength of 424 nm. This suggests that the AgNPs are nearly spherical in shape, as further corroborated by the TEM micrographs displayed in Fig 2. The transmission electron microscopy (TEM) image reveals that the average size of the spherical silver nanoparticles (AgNPs) is approximately 30 ± 5 nm.

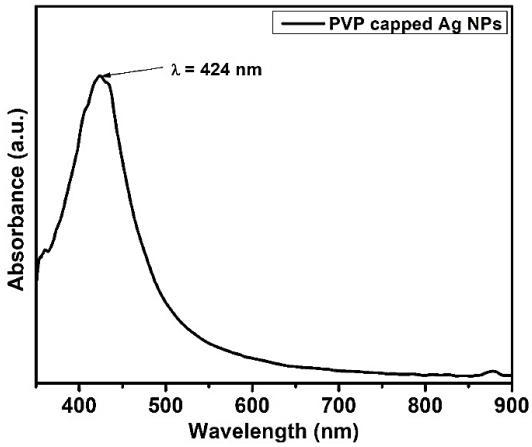


**Fig. 1** UV-Vis absorption spectrum of as-prepared PVP/BH4- capped Ag NPs

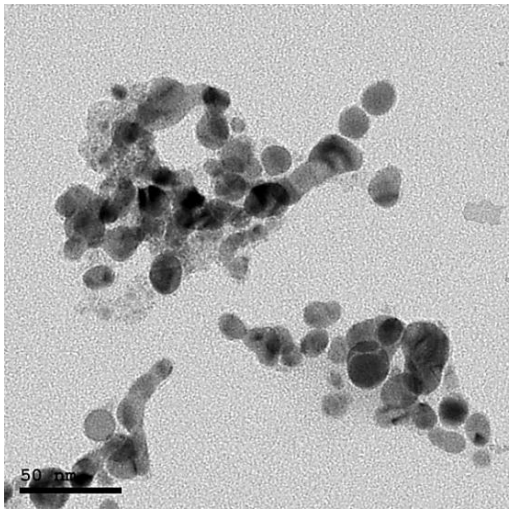


**Fig. 2** TEM image of as-prepared PVP/BH4- capped Ag NPs

Furthermore, the XRD patterns of as-prepared AgNPs' X-ray diffraction (XRD) showed five distinct characteristics. The two most prominent diffraction patterns are observed at an angle of 2θ = 38.27°, which can be attributed to the crystallographic plane (111). The diffraction pattern at an angle of 2θ = 44.47° was attributed to the crystallographic plane (200). Also, the three additional diffraction patterns were acquired at angles of 64.71, 77.73, and 81.9°, respectively. These patterns are reflections from crystallographic planes (220), (311), and (222), which show silver's face-centered cubic (fcc) structure (Ag, Fm-3m (225)). See Fig. 3.

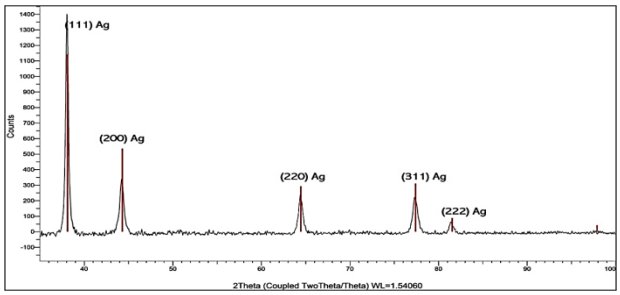


**Fig. 3** XRD patterns of as-prepared PVP/BH4- capped Ag NPs

Finally, the surface and colloidal properties of as-prepared PVP/BH4 capped AgNPs were investigated via dynamic light scattering (DLS) and zeta potential measurements (Fig. 4). The average vesicle size (i.e., Hydrodynamic diameter, HD) was about 57.25 ± 24.75 nm. The polydispersity index (PDI) was about 0.368 (Fig. 4a). Furthermore, the zeta potential of AgNPs shows moderate stability with value of -22 mV (Fig. 4b).

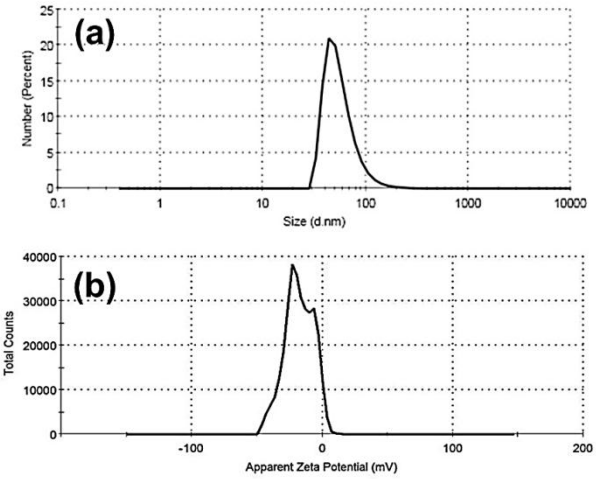


**Fig. 4 (**a) DLS and (b) zetapotential data of as-prepared PVP/BH4- capped AgNPs

Whereas $TiO_2$NPs were prepared by the wet chemical method, they were successfully synthesized via the sol–gel method [29, 30].

$TiO_2$NPs have been prepared at room temperature (25 °C) by hydrolyzing titanium precursors in an alcoholic medium like ethanol or propanol, resulting in the formation of titanium hydroxide. After mixing for 20 min, the gel solution was formed, followed by aging. Then the sol-gel dried and calcined at a known temperature within the range of 400 to 700 °C, depending on the desired crystallographic structure [29, 30]. Fig. 5 illustrates the optical properties of the as-prepared $TiO_2$NPs. The UV-Vis absorption spectrum showed a single narrow absorption band at 280 nm, indicating the formation of TiO2, which is consistent with previous studies [38].

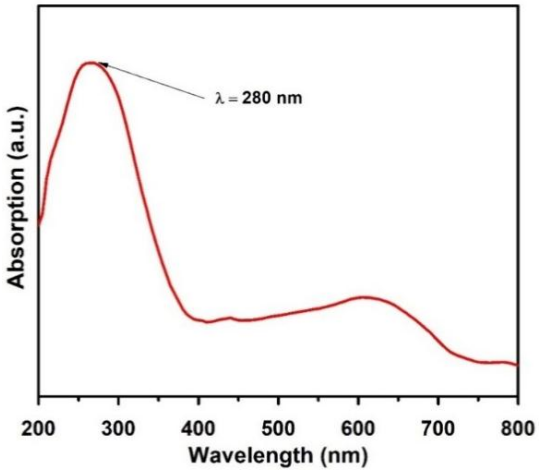


**Fig. 5** Ultraviolet–visible spectroscopy absorption spectrum of as-prepared TiO2NPs

Also, the morphological properties have been confirmed using TEM micrographs, as shown in Fig. 6. The TEM image shows the average size of $TiO_2$NPs were around 20 ± 5 nm with a spherical nanoparticle (See Fig. 6).

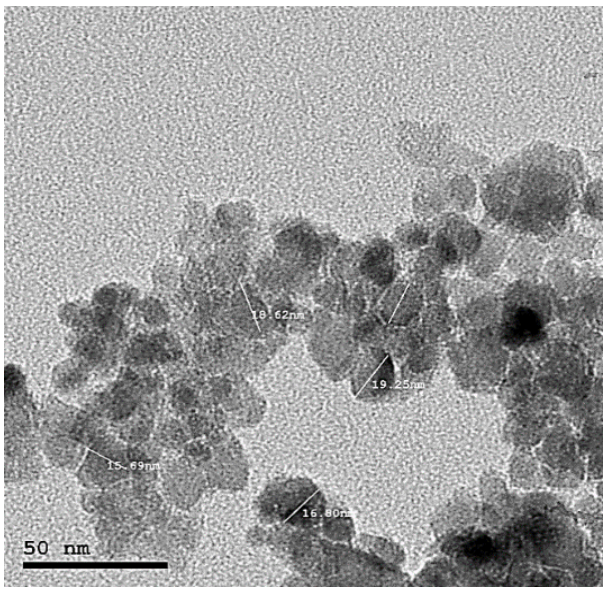


**Fig. 6** TEM image of as-prepared $TiO_2$NPs

Figure 7 showed the crystallographic structure of as-prepared $TiO_2$NPs. Four distinct features characterized by anatase crystallographic structure were monitored at 2θ = 25.3°, which is due to the (101) crystallographic plan. Also, a diffraction pattern at 2θ = 38.47° is assigned to the (004) crystallographic plan. Moreover, another three diffraction patterns obtained at 2θ = 48, and 55.2°, which can be assigned to the reflections from (200), (211), respectively

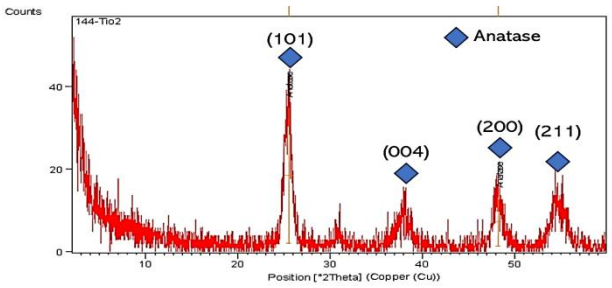


**Fig. 7** XRD patterns of as-prepared $TiO_2$NPs

Finally, the surface and colloidal properties of as-prepared $TiO_2$NPs were investigated via dynamic light scattering (DLS) and zeta potential measurements (Fig. 8). The average vesicle size (i.e., Hydrodynamic diameter, HD) was about 38.04 ± 3.946 nm. The polydispersity index (PDI) was about 1.00 (Fig. 8a). Furthermore, the zeta potential exhibits a moderate stability with value of -9.27 mV (Fig. 8b)

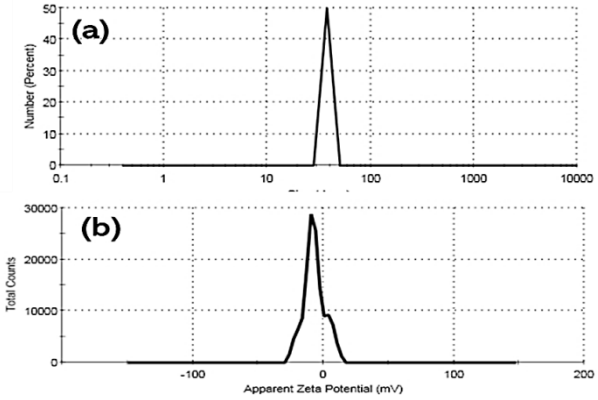


**Fig. 8** (a) DLS and (b) zetapotential data of as-prepared $TiO_2$NPs

**Determination of minimum inhibitory concentration (MIC) of Silver and Titanium nanoparticles against multi-drug-resistant bacterial isolates**

Twenty-two MDR Isolates were inhibited with AgNPs and $TiO_2$NPs MIC through 96 well ELISA plates. MIC of AgNPs was 4ug/ml (Fig 9). On the other hand, the MIC of $TiO_2$NPs was 500 – 1000 µg/mL, while MBC was 1000 µg/mL as in (Fig10).

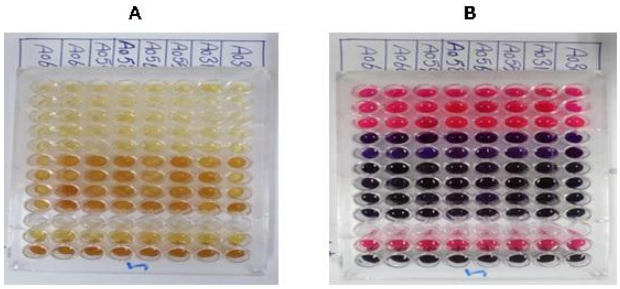


**Fig. 9** Determination of MIC and MBC of AgNPs on tested bacterial isolates through 96 well ELISA plate, where (A) wells with bacterial fermentation without dye, (B) wells with bacterial fermentation with dye after incubation

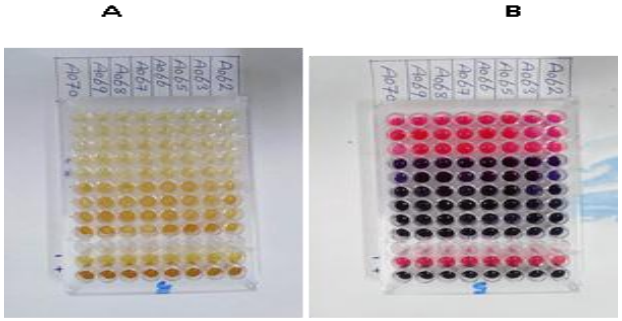


**Fig.10** Determination of MIC and MBC of TiO2 on tested bacterial isolates through 96 well ELISA plate, where (A) wells with bacterial fermentation without dye, (B) wells with bacterial fermentation after incubation with dye.

**The antimicrobial activity of silver and titanium nanoparticles against multi drug resistant isolates**

The MIC and MBC of AgNPs were tested against 22 isolates (Table S-1). Two isolates, *Klebsiella pneumonia* A031 and *Pseudomonas aeruginosa* A065, achieved the highest inhibition zone of 32 mm, while three isolates, *Klebsiella pneumonia* A063, *Klebsiella pneumoniae* A066, and *Klebsiellapneumoniae* A070, achieved an inhibition zone diameter of 31 mm, as shown in Fig. 11. It was also found that microbes like *Streptococcus sp., Bacillus sp., Staphylococcus sp., Shigella sp., Escherichia coli, Pseudomonas aeruginosa, Klebsiella sp.*, and *Candida sp.* did not grow as much when they were treated with AgNPs at a concentration of 1 µg/ml [39]. Significant antibacterial efficacy of AgNPs against pathogenic microorganisms *Pseudomonas aeruginosa* and *Enterobactercloacae*was demonstrated through their growth curve dynamics revealed that as the concentration of nanoparticles increased, the bacterial growth curve's slope steadily declined. Additionally, AgNPs' antibiofilm activity was assessed, and the findings demonstrated that the AgNPs had strong biofilm suppression effect against *Staphylococcus aureus*, *Bacillus subtilis*, and *Pseudomonas aeruginosa*.[17].

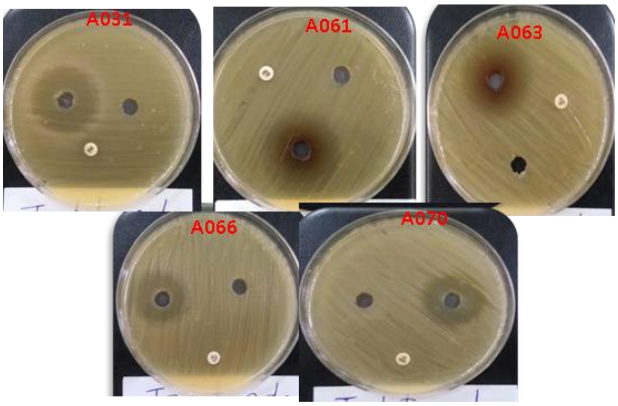


**Fig. 11** Inhibition zone through agar well diffusion method on Muller Hiton with MIC of Ag NPs on extensive five MDR isolates

$TiO_2$NPs with an MIC of 500 to 1000 µg/ml had the best second-line antibacterial activity (Fig. 12). It had the largest clear zone diameter (33 mm) with *Klebsiellapneumoniae* A065, and the next largest was 32 mm with a different isolate of *Klebsiellapneumoniae* A056. Other isolates were stoppedwhen the zone diameter was less than 30 mm, and the MBC of $TiO_2$NPs was found to be 1000 ɛg/ml (Fig. 10 and Table S-1). When both nanoparticles (Ag and TiO2) were at their highest concentration of 1.0 mg/mL (1000µg/mL), they were able to effectively kill these bacteria, our results also agreed with results of [40] who reported that zone of inhibition recorded 31 mm, at 4 mg/mL MIC of and 8 mg/mL MBC of AgNPs to *Staphylococcus aureus* (OR648079), *Aspergillusniger* (OR648075) came next, exhibiting a 30 mm inhibition zone at a minimum fungicidal concentration of 32 mg/mL and a MIC of 16 mg/mL. Then, at a MIC of 8 mg/mL and an MBC of 16 mg/mL, *Enterococcus faecalis* (OR648078), *Klebsiella pneumoniae* (OR648081), and *Acinetobacter baumannii* (OR648080) each showed a 29 mm zone of inhibition. Candida auris (OR648076) showed the least inhibition, with a 25 mm inhibition zone at MIC 16 mg/mL and MFC 32 mg/mL.AgNPs were also shown to have strong biofilm-suppression efficacy to *Pseudomonas aeruginosa*, *Bacillus subtilis*, and *Staphylococcus aureus* [40].


**Fig. 12.** Inhibition zone through agar well diffusion method on Muller Hinton with minimum inhibition concentration of titanium nanoparticles on multi-drug-resistant isolates

AgNPs at its MIC 4 µg/ml and MBC 8 µg/ml were the best antibacterials against 22 isolates; they had the highest inhibition zone (32 mm) with three isolates (13.6%). *Klebsiella pneumoniae* A31, *pseudomonas aeruginosa* A61, *Klebsiella pneumoniae* A65, followed by three isolates (13.6%) with a 31 mm inhibition zone *Klebsiella pneumoniae* A063 and *Klebsiella pneumoniae* A066 and *Klebsiella pneumoniae* A070, followed by three isolates (13.6%) with a 29 mm inhibition zone: *E. coli* A055 inhibition, *Klebsiella pneumoniae* A58, and *Pseudomonas aeruginosa* A069. Other isolates (59%) showed an inhibition zone when treated with AgNPs, but it was less than 29 mm. $TiO_2$NPs at MIC 500 µg/ml and MBC 1000 µg/ml showed inhibition zone 33 mm with one isolate only *Klebsiella Pneumonia* A065 (4.5%), then at MIC and MBC 1000 µg/ml recorded 32 mm inhibition zone with one only *Klebsiella pneumonia* A056 (4.5%), while other isolates were inhibited with inhibition zone less than 30 mm where represent (0.9%) at MBC 1000 µg/ml while differ in MIC between 500 and 1000 µg/ml (Table S-1). The results indicate a significant variation in susceptibility among the different isolates of *Klebsiella pneumoniae*. Furthermore, the inhibition zones found suggest that the higher concentrations of the compounds being tested may be needed to get effective antimicrobial activity against the remaining isolates.

The results of this study clearly demonstrated AgNPs' superior antimicrobial efficacy for MDR bacterial 4isolates compared to $TiO_2$NPs. Because the MIC and MBC values for AgNPs are much lower and they can create larger inhibition zones against a wider range of isolates, these particles are the best antimicrobials available. AgNPs' multiple mechanisms of action, including disruption of the bacterial cell wall, interference with different enzyme functions, and generation of reactive oxygen species, account for their high effectiveness. These results are in concurrence with earlier research; for example, Alsamman et al. reported that the MIC values against various strains of bacteria for AgNPs agreed within the same range noted in our findings. Additionally, Alsamman*et al.* observed that the type of nanoparticle affected the inhibition of global MDR bacterial growth differently [40]. Loo et al. [39] also reported that AgNPs were effective against *Escherichia coli*, *Klebsiella pneumoniae*, *Salmonella typhimurium*, and *Salmonella enteritidis* at MICs of 7.8 µg/mL, 3.9 µg/mL, 3.9 µg/mL, and 3.9 µg/mL.Mekky and co-workers demonstrated in another study the inhibitory action of AgNPs against *Staphylococcus aureus* (OR648079) at the same MIC as the current work, with an inhibition zone of 31 mm at MIC of 4 mg/mL and a minimum bactericidal concentration (MBC) of 8 mg/mL [41].

Additionally, AgNPs, at a concentration of 3 mg/mL, significantly fragmented DNA in all bacterial strains, except for *Enterococcus faecalis*[42]. Lemon extract [L-AgNPs] and pomegranate extract [P-AgNPs] were used as starting materials to produce silver nanoparticles. The dosages of both extracts were assessed at different levels: 50, 30, 15, 7, and 5 µg/mL. The minimum inhibitory concentration (MIC) for [L-AgNPs] was 50 µg/mL. It was found that 30 µg/mL of [P-AgNPs] was the minimum concentration needed to stop the growth of *E. coli*, *Enterococcus faecalis*, *Acinetobacter baumannii*, and *Klebsiella pneumonia* [42]. The inhibition zone widths for these bacteria were measured to be 11, 15, 12, and 13 mm, respectively, at the MIC of L-AgNPs. MICs of P-AgNPs against *Enterococcus faecalis, Pseudomonas aeruginosa, Acinetobacter baumannii, and Klebsiella pneumoniae* were found to be 13, 16, 9, and 9 mm, respectively [42].

**Table S-1** Comparing the antibacterial effects of Silver and titanium nanoparticles on multi-drug resistant β hemolytic isolates

| | Isolate | Clear zone | | (MIC) | | MBC | |
|---|---|---|---|---|---|---|---|
| | | AgNPs | $TiO_2$ NPs | Ag NPs | $TiO_2$ NPs | AgNPs | $TiO_2$ NPs |
| 1 | ***Klebsiella Pneumonia* A020** | 19 | 20 | 4 | 500 | 8 | 1000 |
| 2 | ***AcinetobacterBaumannii*A022** | 24 | 23 | 4 | 1000 | 8 | 1000 |
| 3 | ***Pseudomonas Aeruginosa*A023** | 28 | 24 | 4 | 1000 | 8 | 1000 |
| 4 | ***Klebsiella Pneumonia* A025** | 22 | 23 | 4 | 500 | 8 | 1000 |
| 5 | ***Klebsiella Pneumonia* A026** | 26 | 24 | 4 | 500 | 8 | 1000 |
| 6 | ***Klebsiella Pneumonia* A027** | 22 | 22 | 4 | 500 | 8 | 1000 |
| 7 | ***Klebsiella Pneumonia* A030** | 21 | 22 | 4 | 500 | 8 | 1000 |
| 8 | ***Klebsiella Pneumonia* A031** | 32 | 26 | 4 | 500 | 8 | 1000 |
| 9 | ***E. coli* A055** | 29 | 23 | 4 | 500 | 8 | 1000 |
| 10 | ***Klebsiella Pneumonia* A056** | 23 | 32 | 4 | 1000 | 8 | 1000 |
| 11 | ***Klebsiella Pneumonia* A058** | 29 | 25 | 4 | 500 | 8 | 1000 |
| 12 | ***Klebsiella Pneumonia* A059** | 28 | 23 | 4 | 500 | 8 | 1000 |
| 13 | ***Klebsiella Pneumonia* A060** | 27 | 22 | 4 | 500 | 8 | 1000 |
| 14 | ***Pseudomonas Aeruginosa*A061** | 32 | 29 | 4 | 1000 | 8 | 1000 |
| 15 | ***Klebsiella Pneumonia* A062** | 29 | 24 | 4 | 500 | 8 | 1000 |
| 16 | ***Klebsiella Pneumonia* A063** | 31 | 25 | 4 | 500 | 8 | 1000 |
| 17 | ***Klebsiella Pneumonia* A065** | 32 | 33 | 4 | 500 | 8 | 1000 |
| 18 | ***Klebsiella Pneumonia* A066** | 31 | 24 | 4 | 500 | 8 | 1000 |
| 19 | ***Klebsiella Pneumonia* A067** | 26 | 25 | 4 | 500 | 8 | 1000 |
| 20 | ***Klebsiella Pneumonia* A068** | 26 | 24 | 4 | 500 | 8 | 1000 |
| 21 | ***Pseudomonas Aeruginosa*A069** | 29 | 22 | 4 | 1000 | 8 | 1000 |
| 22 | ***Klebsiella Pneumonia* A070** | 31 | 23 | 4 | 500 | 8 | 1000 |

Summary of statistical analysis of nanoparticles result was mentioned in Table 2, in which AgNPs showed mean of inhibitory zone diameter 27.1 against $TiO_2$NPs with 24.4, also median values were 28, and 24 respectively. Besides that,Confidence Level (95.0%) was 1.7 and 1.4 with AgNPs and $TiO_2$NPs, respectively.

**Table 2.** statistical analysis of two NPs AgNPs and $TiO_2$ NPs through ANOVA

| | AgNPs | $TiO_2$ NPs |
|---|---|---|
| Mean | 27.1 | 24.4 |
| Standard Error | 0.830416 | 0.673324 |
| Median | 28 | 24 |
| Mode | 29 | 23 |
| Standard Deviation | 3.894996 | 3.158168 |
| Sample Variance | 15.171 | 9.974026 |
| Kurtosis | -0.73114 | 2.617289 |
| Skewness | -0.5331 | 1.643473 |
| Range | 13 | 13 |
| Minimum | 19 | 20 |
| Maximum | 32 | 33 |
| Sum | 597 | 538 |
| Count | 22 | 22 |
| Largest(1) | 32 | 33 |
| Smallest(1) | 19 | 20 |
| Confidence Level(95.0%) | 1.726945 | 1.400253 |

While less effective overall, $TiO_2$NPs still proved significant antibacterial activity, particularly against certain *Klebsiellapneumoniae* strains. The fact that $TiO_2$NPs need higher concentrations to work as an inhibitor suggests a different way they work, which may have something to do with their photocatalytic properties and the production of ROS. The variation in effectiveness between different bacterial species and strains underscores the importance of considering the specific pathogen when selecting nanoparticle-based treatments. When it came to killing MDR bacteria, biosynthesized $TiO_2$NPs were the most effective nanoparticle type, followed by AgNPs[43]. At the highest concentration of 1.0 mg/mL (1000µg/mL) of both nanoparticles (Ag and TiO2), they were effective at killing these bacteria. However, at concentrations of 0.75 mg/mL, 0.5 mg/mL, and 0.25 mg/mL, the inhibitory effect was less effective [43]. The most effective way to stop Bacillus subtlis and Bacillus anthracis from growing was with Ag and $TiO_2$NPs, more effective than the standard drug (Ciprofloxacin injection). However, $TiO_2$NPs showed outstanding antibacterial properties that were better than Ag NPs. AgNPs showed the most minor activity against *E. coli*, while $TiO_2$NPs showed the most minor activity against Staphylococcus aureus [43].

Also, the lowest concentrations (MICs) of AgNPs and $TiO_2$NPs made by microorganisms were 3 µg (67.2 µg/mL) for AgNPs and 9 µg (180 µg/mL) for $TiO_2$NPs [44]. The concentrations we employed, namely 4 µg/mL and 8 µg/mL with AgNPs and $TiO_2$NPs, respectively, were lower than these amounts. AgNPs had the greatest total and mean values compared to other types of nanoparticles, according to ANOVA analysis. Similarly, we selected the nanoparticles with the highest effectiveness to determine MIC value against the most vulnerable bacteria. It was found that 15 µg of AgNPs (equal to 300 µg/ml) was the lowest concentration that could stop the growth of isolate 5. The lowest concentration that could stop the growth of isolate 27 was 18.75 µg (equal to 375 µg/ml) [44].

## In-vitro cytotoxicity

The different concentrations of AgNPs and $TiO_2$NPs were tested against hepatocarcinoma cells (HepG-2), where AgNPs showed remarked toxicity of 15 % at a dose of 62.5 µg/ml. The toxicity directly increases with concentration. Other concentrations were recorded at 68.1 % at 125 µg/ml, then 86.4% at 250 ug/ml, and 92.5% at 500 µg/ml. Finally, it retched 96.2 at 1000 µg/ml. AgNPs were applied at IC50 (102 µg/ml). $TiO_2$NPs had less toxicity on the same types of HepG-2 cells, as toxicity appeared at a concentration higher than 125 µg/ml; it was 3.2% at 250 µg/ml, then 28.2% at 500 µg/ml, and finally 90.2% at 1000 µg/ml with an IC50 of 663.3 µg/ml. (See Fig 13 and 14).

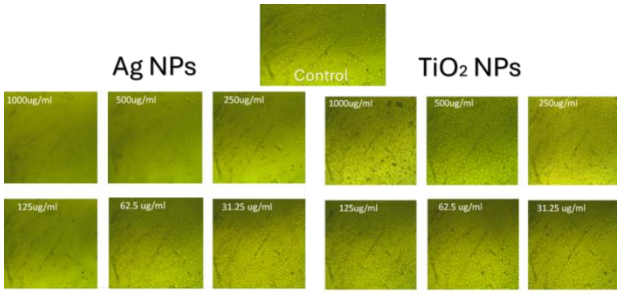


**Fig. 13** Antineoplastic activity of silver and titanium nanoparticles to HepG2 cell line at different concentrations against a control sample.

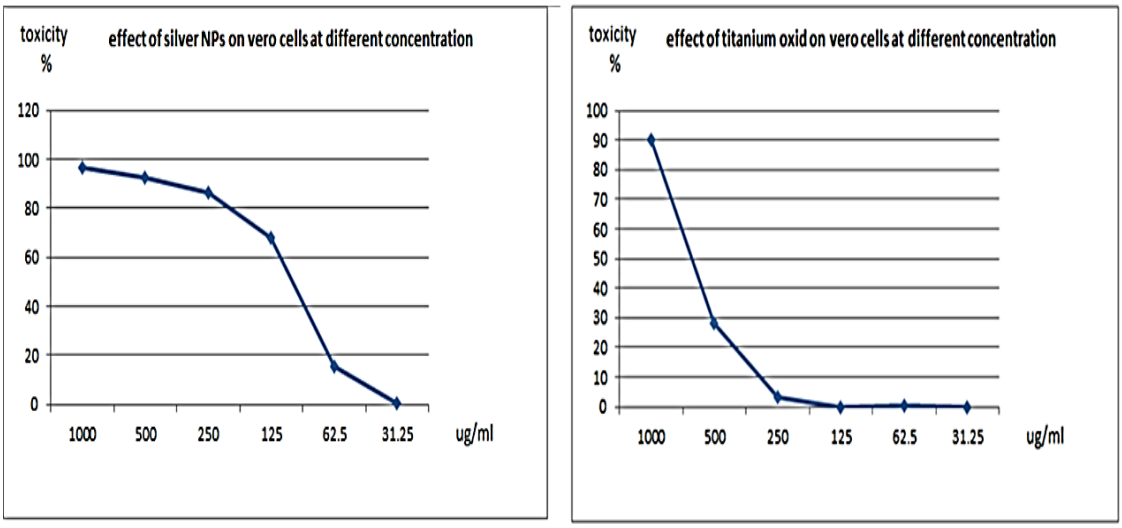


**Fig. 14** Cytotoxic effect of Ag and TiO2 NPs to HepG2 cell line at different concentrations against control sample

## Conclusion

We investigated the optical, morphological structure, and colloidal properties of AgNPs and $TiO_2$NPs using UV-Vis absorption spectroscopy, transmission electron microscopy (TEM), X-ray diffraction analysis (XRD), and dynamic light scattering (DLS) techniques. The average particle size of these NPs is 30±5 nm for AgNPs and 20±5 nm for $TiO_2$NPs. The crystal structures of the AgNPs and $TiO_2$NPs are cubic and anatase, respectively. Synthesized AgNPs and $TiO_2$NPs demonstrated antibacterial activity against urinary tract bacterial strains. *Klebsiella pneumonia*, especiallyagainst the most extensive MDR bacterial strains, was *Klebsiella pneumonia*A031 [OP811040] and *Klebsiella pneumonia*A065 [OP811041] ata minimal inhibition concentration (MIC) within the range of 4 to 8 µg/mL in the case of AgNPs, and 500 to 1000 µg/mL of $TiO_2$NPs.

## Financial support and sponsorship

Nil.

## Authors' contributions

**AA**, conceptualization, writing review, methodology, resources, investigation, and writing an original draft. **ANE**, biosynthesis and characterization of tested nanoparticles, resources, supervision, writing and revision of an original manuscript draft. **ESA**, conceptualization, methodology. **EAE**, resources, supervision, and writing review. **MK**, conceptualization, writing review, methodology, resources, investigation, and writing original draft methodology. The authors read and approved the final manuscript.

## Availability of data and material

The datasets used and analyzed during the current study are available from the corresponding author on reasonable request.

## Conflicts of interest

There are no conflicts of interest.

## References

1. Infectious Diseases Society OF America (IDSA). Combating antimicrobial resistance: policy recommendations to save lives. *Clinical Infectious Diseases*, 2011; 52.suppl_5: S397-S428.
2. K.Z. Vardakas, P.I. Rafailidis, A.A. Konstantelias, M.E. Falagas, Predictors of mortality in patients with infections due to multi-drug resistant Gram negative bacteria: the study, the patient, the bug or the drug?, Journal of Infection, 2013; 66: 401-414.
3. M. Bodi, C. Ardanuy, J. Rello, Impact of Gram-positive resistance on outcome of nosocomial pneumonia, Critical care medicine, 2001; 29: N82-N86.
4. F. Perez, D. Van Duin, Carbapenem-resistant Enterobacteriaceae: a menace to our most vulnerable patients, Cleveland Clinic journal of medicine, 2013; 80: 225.
5. B. Foxman, The epidemiology of urinary tract infection, Nature Reviews Urology, 2010; 7: 653-660.
6. C.B. Chibelean, R.-C. Petca, C. Mareș, R.-I. Popescu, B. Enikő, C. Mehedințu, A. Petca, A clinical perspective on the antimicrobial resistance spectrum of uropathogens in a Romanian male population, Microorganisms, 2020; 8: 848.
7. F.M. Wagenlehner, T.E. Bjerklund Johansen, T. Cai, B. Koves, J. Kranz, A. Pilatz, Z. Tandogdu, Epidemiology, definition and treatment of complicated urinary tract infections, Nature Reviews Urology, 2020; 17: 586-600.
8. J.S. Weese, J. Blondeau, D. Boothe, L.G. Guardabassi, N. Gumleyg, M. Papichh, L.R. Jesseni, M. Lappinj, S. Rankin, J.L. Westropp, International Society for Companion Animal Infectious Diseases (ISCAID) guidelines for the diagnosis and management of bacterial urinary tract infections in dogs and cats, Journal of Japanese Association of Veterinary Nephrology and Urology, 2021; 13: 46-63.

9. A.L. Flores-Mireles, J.N. Walker, M. Caparon, S.J. Hultgren, Urinary tract infections: epidemiology, mechanisms of infection and treatment options, Nature reviews microbiology, 2015; 13: 269-284.
10. R.D. Klein, S.J. Hultgren, Urinary tract infections: microbial pathogenesis, host–pathogen interactions and new treatment strategies, Nature Reviews Microbiology, 2020; 18: 211-226.
11. S.V. Sánchez, N. Navarro, J. Catalán-Figueroa, J.O. Morales, Nanoparticles as potential novel therapies for urinary tract infections, Frontiers in cellular and infection microbiology, 2021; 11: 656496.
12. M. Qindeel, M. Barani, A. Rahdar, R. Arshad, M. Cucchiarini, Nanomaterials for the diagnosis and treatment of urinary tract infections, Nanomaterials, 2021; 11: 546.
13. T.C. Dakal, A. Kumar, R.S. Majumdar, V. Yadav, Mechanistic basis of antimicrobial actions of silver nanoparticles, Frontiers in microbiology, 2016; 7: 1831.
14. H.R. Ali, A.N. Emam, E.G. Hefny, N.F. Koraney, A.S. Mansour, A.M. Salama, S.F. Ali, S.H. Aboolo, M.A. Shahein, Silver nanoparticles enhance the effectiveness of traditional antibiotics against S. aureus causing bovine mastitis within the safety limit, Journal of Nanoparticle Research, 2021; 23: 1-18.
15. N. El-Kattan, A.N. Emam, A.S. Mansour, M.A. Ibrahim, A.B. Abd El-Razik, K.A. Allam, N.Y. Riad, S.A. Ibrahim, Curcumin assisted green synthesis of silver and zinc oxide nanostructures and their antibacterial activity against some clinical pathogenic multi-drug resistant bacteria, RSC advances, 2022; 12: 18022-18038.
16. H.R. Ali, A.N. Emam, N.F. Koraney, E.G. Hefny, S.F. Ali, Combating the prevalence of water-borne bacterial pathogens using anisotropic structures of silver nanoparticles, Journal of Nanoparticle Research, 2020; 22: 1-15.
17. A.A. Hamed, H. Kabary, M. Khedr, A.N. Emam, Antibiofilm, antimicrobial and cytotoxic activity of extracellular green-synthesized silver nanoparticles by two marine-derived actinomycete, RSC advances, 2020, 10: 10361-10367.
18. E. Ghazy, A. Kumar, M. Barani, I. Kaur, A. Rahdar, T. Behl, Scrutinizing the therapeutic and diagnostic potential of nanotechnology in thyroid cancer: Edifying drug targeting by nano-oncotherapeutics, Journal of Drug Delivery Science and Technology, 2021; 61: 102221.
19. J. Dubey, A. Singh, Green synthesis of TiO2 nanoparticles using extracts of pomegranate peels for pharmaceutical application, International Journal of Pharmaceutical and Phytopharmacological Research, 2019; 9: 85-87.
20. U.L. Ifeanyichukwu, O.E. Fayemi, C.N. Ateba, Green synthesis of zinc oxide nanoparticles from pomegranate (Punica granatum) extracts and characterization of their antibacterial activity, Molecules, 2020; 25: 4521.
21. A. Abdal Dayem, M.K. Hossain, S.B. Lee, K. Kim, S.K. Saha, G.-M. Yang, H.Y. Choi, S.-G. Cho, The role of reactive oxygen species (ROS) in the biological activities of metallic nanoparticles, International journal of molecular sciences, 2017, 18: 120.
22. A.A. Khan, A.M. Alanazi, N. Alsaif, T.A. Wani, M.A. Bhat, Pomegranate peel induced biogenic synthesis of silver nanoparticles and their multifaceted potential against intracellular pathogen and cancer, Saudi Journal of Biological Sciences, 2021; 28: 4191-4200.
23. N.M. Hawsawi, A.M. Hamad, S.N. Rashid, F. Alshehri, M. Sharaf, S.A. Zakai, S.A. Al Yousef, A.M. Ali, A. Abou-Elnour, A. Alkhudhayri, Biogenic silver nanoparticles eradicate of Pseudomonas aeruginosa and Methicillin-resistant Staphylococcus aureus (MRSA) isolated from the sputum of COVID-19 patients, Frontiers in Microbiology, 2023; 14: 1142646.
24. N. Dasgupta, C. Ramalingam, Silver nanoparticle antimicrobial activity explained by membrane rupture and reactive oxygen generation, Environmental chemistry letters, 2016; 14: 477-485.
25. P. Patel, J. Vadalia, K. Butani, K. Jadwani, N.K. Mandal, L. Khodaie, Green synthesis of silver nanoparticles, characterization and their biological efficacy, Nanotechnology and In Silico Tools, 2024; 117-139.
26. V. Verma, M. Al-Dossari, J. Singh, M. Rawat, M.G. Kordy, M. Shaban, A review on green synthesis of TiO2 NPs: photocatalysis and antimicrobial applications, Polymers, 2022; 14:1444.
27. M. Schutte-Smith, E. Erasmus, R. Mogale, N. Marogoa, A. Jayiya, H. Visser, Using visible light to activate antiviral and antimicrobial properties of TiO2 nanoparticles in paints and coatings: focus on new developments for frequent-touch surfaces in hospitals, Journal of coatings technology and research, 2023; 1-29.
28. C.L. de Dicastillo, M.G. Correa, F.B. Martínez, C. Streitt, M.J. Galotto, Antimicrobial effect of titanium dioxide nanoparticles, Antimicrobial Resistance-A One Health Perspective, 2020.
29. W. Buraso, V. Lachom, P. Siriya, P. Laokul, Synthesis of TiO2 nanoparticles via a simple precipitation method and photocatalytic performance, Materials Research Express, 2018; 5: 115003.
30. P. Praveen, G. Viruthagiri, S. Mugundan, N. Shanmugam, Sol–gel synthesis and characterization of pure and manganese doped TiO2 nanoparticles–A new NLO active material, Spectrochimica Acta Part A: Molecular and Biomolecular Spectroscopy, 2014; 120: 548-557.
31. A. Logan, Bacillus and recently derived genera, Manual of clinical microbiology, 1999; 357-369.
32. J.G. Cappuccino, Mi cr obiolo gy A laboratory manual, 2018.
33. A. Mostafaei, Application of multivariate statistical methods and water-quality index to evaluation of water quality in the Kashkan River, Environmental Management, 2014; 53: 865-881.
34. T. Mosmann, Rapid colorimetric assay for cellular growth and survival: application to proliferation and cytotoxicity assays, Journal of immunological methods, 1983; 65: 55-63.
35. N.P. Vidal, C.F. Manful, T.H. Pham, P. Stewart, D. Keough, R. Thomas, The use of XLSTAT in conducting principal component analysis (PCA) when evaluating the relationships between sensory and quality attributes in grilled foods, MethodsX, 2020; 7; 100835.
36. S. Singh, A. Bharti, V.K. Meena, Green synthesis of multi-shaped silver nanoparticles: Optical, morphological and antibacterial properties, Journal of Materials Science: Materials in Electronics, 2015; 26: 3638-3648.
37. L. Mulfinger, S.D. Solomon, M. Bahadory, A.V. Jeyarajasingam, S.A. Rutkowsky, C. Boritz, Synthesis and study of silver nanoparticles, Journal of chemical education, 2007; 84: 322.
38. A.K. Shimi, H.M. Ahmed, M. Wahab, S. Katheria, S.M. Wabaidur, G.E. Eldesoky, M.A. Islam, K.P. Rane, Synthesis and applications of green synthesized TiO 2 nanoparticles for photocatalytic dye degradation and antibacterial activity, Journal of Nanomaterials, 2022.
39. Y.Y. Loo, Y. Rukayadi, M.-A.-R. Nor-Khaizura, C.H. Kuan, B.W. Chieng, M. Nishibuchi, S. Radu, In vitro antimicrobial activity of green synthesized silver nanoparticles against selected gram-negative foodborne pathogens, Frontiers in microbiology, 2018; 9: 1555.
40. A.M. Alsamman, M. Khedr, H.A. Kabary, M. El-Sehrawy, Elimination of pathogenic multidrug resistant isolates through different metal oxide nanoparticles synthesized from organic plant and microbial sources, Microbial Pathogenesis, 2023; 178: 106055.
41. A.E. Mekky, A.E. Abdelaziz, F.S. Youssef, S.A. Elaskary, A.A. Shoun, E.A. Alwaleed, M.A. Gaber, A.A. Al-Askar, A.M. Alsamman, A. Yousef, Unravelling the

Antimicrobial, Antibiofilm, Suppressing Fibronectin Binding Protein A (fnba) and cna Virulence Genes, Anti-Inflammatory and Antioxidant Potential of Biosynthesized Solanum lycopersicum Silver Nanoparticles, Medicina, 2024; 60: 515.

42. M. Abdelrazik, H.H. Elkotaby, A. Yousef, A.F. El-Sayed, M. Khedr, Green synthesis of silver nanoparticles derived from lemon and pomegranate peel extracts to combat multidrug-resistant bacterial isolates, Journal of Genetic Engineering and Biotechnology, 2023; 21: 97.
43. A.A. Jimoh, B.H Akpeji, S.O. Azeez, Y.O. Ayipo, Z.A. Abdulsalam, Z.F. Adebayo, A.T. Ajao, A.T. Zakariyah, E.E. Elemike, Biosynthesis of Ag and TiO2 nanoparticles and the evaluation of their antibacterial activities. Inorganic Chemistry Communications, 2022; 141: 109503.
44. P. Shakib, R. Saki, A. Marzban, G. Goudarzi, S. Ghotekar, K. Cheraghipour, M.R. Zolfaghari, Antibacterial Effects of Nanocomposites on Efflux Pump Expression and Biofilm Production in Pseudomonas aeruginosa: A Systematic Review, Current Pharmaceutical Biotechnology, 2024; 25: 77-92.
45. V. Kumar, N. Sharma, S. Maitra, In vitro and in vivo toxicity assessment of nanoparticles, International Nano Letters, 2017; 7: 243-256.
46. K. Priya, M. Vijayakumar, B. Janani, Chitosan-mediated synthesis of biogenic silver nanoparticles (AgNPs), nanoparticle characterisation and in vitro assessment of anticancer activity in human hepatocellular carcinoma HepG2 cells, International journal of biological macromolecules, 2020; 149: 844-852.
47. M. Younas, M. Rizwan, M. Zubair, A. Inam, S. Ali, Biological synthesis, characterization of three metal-based nanoparticles and their anticancer activities against hepatocellular carcinoma HepG2 cells, Ecotoxicology and Environmental Safety, 2021; 223: 112575.